

QUT Digital Repository:  
<http://eprints.qut.edu.au>



Huang, Ming-Hui and Thambiratnam, David P. and Perera, Nimal J. (2005)  
Resonant vibration of shallow suspension footbridges. *Proceedings of ICE, Bridge Engineering* 158(BE4):pp. 201-209.

© Copyright 2005 Thomas Telford (Institution of Civil Engineers, UK)

# Resonant Vibration of Shallow Suspension Footbridges with Coupled Modes under Walking Loads

Ming –Hui Huang<sup>1\*</sup>, David P. Thambiratnam<sup>2</sup> and Nimal J. Perera<sup>3</sup>

<sup>1</sup> PhD Candidate, School of Urban Development, Queensland University of Technology, GPO Box 2434, Brisbane, Queensland 4001, Australia

<sup>2</sup> Professor, School of Urban Development, Queensland University of Technology, GPO Box 2434, Brisbane, Queensland 4001, Australia

<sup>3</sup> Director, Robert Bird & Partners, Brisbane, Queensland 4000, Australia

\* Corresponding author, Email Address: [m2.huang@qut.edu.au](mailto:m2.huang@qut.edu.au), Phone: 61-7-3864 2046, Fax: 61-7-3864 1170

## Abstract

A cable supported footbridge model with pre-tensioned cables in vertical and horizontal planes is proposed to investigate the vibration characteristics of shallow suspension footbridges under walking dynamic loads in this conceptual study. In this bridge model, the tension force in the supporting cables can be adjusted by introducing pre-tensions to the reverse profiled cables, and therefore the natural frequencies can be altered and cover the frequency range of dynamic force induced by pedestrians. In the numerical analysis, SAP2000 is adopted to study the vibration properties and dynamic response under walking loads. The dynamic behaviour of the bridge under structure synchronous excitation is stimulated by resonant vibration. The crowd walking loads are modelled as uniform loads acting on the whole bridge deck and they consist of three parts: vertical dynamic force, lateral dynamic force and vertical static force. Numerical results show that for shallow suspension footbridge the lowest frequencies correspond to lateral and torsional vibration modes which are always combined together and become two types of coupled modes: coupled lateral-torsional modes, as well as coupled torsional-lateral modes. As an example, a bridge model with fundamental frequency of 0.75 Hz in the lateral direction has been studied. It is found that the vibration in lateral direction is quite different from that in the vertical direction and the damping has significant effect on the vertical vibration but small effect on the lateral one. And vertical static load has significant effect on the lateral vibration when the bridge structure vibrated in coupled modes.

**Keywords** footbridge; suspension; pre-tension; coupled modes; crowd; walking; resonance; dynamic response.

## 1 Introduction

Due to the application of light and high strength material, modern footbridges can cross longer spans and be constructed lighter and more slender than ever. However,

slender bridge structures with low stiffness, low structural mass and damping ratio are prone to vibration induced by pedestrians and other human activities<sup>1</sup>.

Recent years, the excessive lateral vibration of footbridges has attracted the attention of researchers and bridge engineers. Although many footbridges have been reported suffering excessive lateral vibration induced by pedestrians, only a few bridges such as T-Bridge in Japan<sup>2-5</sup> and Millennium Bridge in London<sup>6-13</sup> have been extensively investigated. Research shows that when crossing a bridge which is vibrating at a frequency within the range of walking rates, pedestrians tend to change their pacing rates to move in harmony with the bridge vibration. This mechanism leads to large amplitude synchronous vibration, which can cause serious vibration serviceability problems in footbridges. Investigation of Millennium Bridge in London shows that lateral synchronous excitation can be caused by the combination of high pedestrian density and the presence of lateral modes of vibration below 1.3 Hz, independent of the bridge structural forms. Some field measurements<sup>14</sup> on M-bridge in Japan also show that not only the fundamental frequency can be excited by pedestrians, but also higher order vibration modes can be excited depending on the distribution of pedestrians.

However, the behaviour of pedestrians on a vibrating footbridge is quite complicated, and the walking dynamic loads depend not only on the weight of pedestrian, pacing rate and type of footwear, but also on the interaction between pedestrian and the footbridge structure<sup>15</sup>. In general, walking dynamic load has three components in the vertical, lateral and longitudinal directions respectively. In the vertical direction, the dynamic force is generated due to up and down movements as the body passes over a supporting leg and descends as this leg passes behind. In the lateral direction, the forces are caused by the periodic sway of the body weight from one leg to the other. These two aforementioned forces are the ones of most interest as sources of excitation in footbridges although there are forces applied in the longitudinal direction, as well. The vertical component has been investigated well for long time and many load models have been proposed<sup>16-18</sup>, but only a few publications have described the force functions of the lateral and longitudinal components<sup>15, 19</sup>. It seems that further research is needed in order to determine the force functions at different pacing rates.

A conceptual study has been undertaken to investigate the dynamic characteristics of slender footbridges under human-induced dynamic loads and a cable supported bridge model with pre-tensioned reverse profiled cables in the vertical plane and side pre-tensioned cables in the horizontal plane is proposed for this purpose. This paper presents some features of dynamic characteristics of a shallow suspension footbridge with pre-tensioned reverse profiled cables. In the numerical analysis, SAP2000<sup>20</sup> is adopted to study the vibration properties and dynamic response under walking dynamic loads. It is assumed that the walking dynamic loads are distributed uniformly on the bridge deck and different force-time functions in the vertical direction are used based on the pacing rates. In the lateral direction, the force-time function for one foot takes the same pattern as that in vertical direction, but the force value takes 4% of its vertical component. In order to illustrate the dynamic characteristics, a bridge model with fundamental frequency of 0.75 Hz in the lateral direction has been chosen for the non-linear time history dynamic analysis. The feature of resonant vibration under walking dynamic loads is shown. The effect of damping ratio and static weight on the dynamic response are discussed.

## 2 Proposed bridge model

The proposed pre-tensioned cable supported bridge model is shown in Fig. 1. In this bridge model, the cable system is composed of three groups of cables which may have same or different cable profiles: top suspending (or supporting) cables and bottom pre-tensioned cables (Fig. 1(a)) and side pre-tensioned cables (Fig. 1(b)). The top cables are two parallel suspending cables which have the catenary profiles and provide tension forces to support the whole structural gravity, applied loads and extra internal forces induced by the bottom pre-tensioned cables. Two parallel bottom cables are designed to have reverse profiles in the vertical plane and their function is to introduce pre-tension forces and provide extra internal vertical forces to transverse bridge frames and the top suspending cables. The side cables are a pair of bi-concave cables which have the same cable profiles in the horizontal plane, and their main function is to provide extra internal horizontal forces and horizontal stiffness. When the pre-tensioned bottom and/or side cables are slack, they could carry small tension forces only to support their own gravity and cannot resist any external loads. In this case, they will not be able to contribute stiffness and tension forces to the structure. However, these small tensions can provide sufficient restraining forces to prevent the transverse frames from swaying in the longitudinal direction.

Transverse bridge frames have been designed to support the deck and hold the cables. These frames (Fig. 1(c)) comprise cross members (for the support beams and deck), top and bottom vertical legs as well as horizontal side legs and they form a set of spreaders for the cables to create the required profiles. They have in plane stiffness to protect against collapse under in plane forces and contribute very little in the way of longitudinal, lateral and rotational stiffness for the entire system. The transverse bridge frames are hung from the top cables, and further restrained by the lower reversed profile cables as well as the side cables. Two support beams of rectangular section are simply supported on cross members of the adjacent bridge frames, and the deck units are simply supported at the ends on these beams.

In this bridge model, the entire structural stiffness is provided by the cable systems. When the structure is subjected to applied loads, the entire load can be balanced by the tension forces in the cables with deformed cable profiles since these forces can provide components in different directions. In order to simplify the problem, all the transverse bridge frames have been assumed to have the same size, and hence the weight of frame and deck acting on the cables can be considered as equal concentrated loads.

In the analysis of the bridge model, all the cables are stretched to keep the designed cable sags or cable profiles and then the decks can be kept in a horizontal plane. This can be done by introducing initial distortions to the cables based on their cable sags, cross sectional areas, material properties, loads such as the weight of bridge frame and decks as well as cables, and extra internal forces produced by pre-tensioned reverse profiled cables or horizontal side cables.

The structural analysis package SAP2000 was adopted in the numerical study. In the bridge model, stainless steel (Young's modulus  $2.0 \times 10^{11}$  N/m<sup>2</sup> and density 7850

kg/m<sup>3</sup>) was chosen for the transverse bridge frames and support beams, and Aluminium (Young's modulus  $6.5 \times 10^{10}$  N/m<sup>2</sup> and density 2700 kg/m<sup>3</sup>) was chosen for the deck units to reduce the weight of the bridge structure. All members of the transverse bridge frames have a uniform rectangular cross sectional area of 250×300 mm<sup>2</sup> and the support beams have a uniform rectangular cross section of 200×250 mm<sup>2</sup>. 8 deck units with dimensions 4000×500×50 mm<sup>3</sup> are simply supported on the support beams between the adjacent transverse bridge frames. Stainless steel cables are chosen for all the cable systems and the material properties are the same as those of bridge frames. In the numerical analysis, the span length is set to 80m, the horizontal distance between the adjacent bridge frames is set to 4m and the width of the deck for applied loads is set to 4m. All the cable sags are set to 1.8m and diameters of the cables to 240 mm.

### 3 Walking Dynamic Loads

As mentioned before, synchronous excitation can be caused by the combination of high density of pedestrians and low natural frequencies within the frequency range of pacing rate. When synchronization occurred, almost 20 percent of pedestrians completely synchronize their footfalls<sup>2</sup>. The first harmonic of lateral dynamic load factor is reported in the range of 0.03 to 0.1 (about 23 N to 70 N)<sup>21</sup>.

In this paper, the crowded pedestrian loads are modelled as uniformly distributed loads on the entire bridge deck. It is assumed that 20 percent of pedestrians participated fully in the synchronization process and generated vertical and lateral dynamic loads. The remaining 80% pedestrians generate only static vertical load on the bridge deck as they walk with random pacing rates and phases. Wheeler's force functions<sup>16</sup> of one footfall are adopted to model the vertical dynamic walking load. It is assumed that the lateral force of one foot has the same force function as its vertical component, but the magnitude is only a small portion (4%) of the vertical component.

Fig. 2 shows the typical vertical force functions<sup>16</sup> from slow walk to fast walk. It can be seen that the peak value and shape of a force function vary according to pacing rate. However, it should be mentioned that in the reference, the pacing rate of normal walk is greater than that of brisk walk, but its curve is much flatter. In order to model the walking dynamic loads, the walking activities are classified into four types according to their pacing rates and each type of activity covers a range of frequency: slow walk (smaller than 1.8Hz), normal walk (1.8Hz ~ 2.2Hz), brisk walk (2.2-2.7Hz) and fast walk (greater than 2.7Hz).

Taking the normal walk for example, if the force function of one foot is defined as  $F_n[t]$  and the period and foot contact time are  $T_n$  and  $T_{nc}$  (Fig. 3), then this function has the following property:

$$F_n[t] = \begin{cases} 0 & t < 0 \text{ or } t > T_{nc} \\ F_n[t] & 0 \leq t \leq T_{nc} \end{cases} \quad (1)$$

Therefore, the continuous vertical force function  $F_{nv}(t)$  and lateral force function  $F_{nl}(t)$  can be expressed according the pacing rate ( $f_p$ ) or load period ( $T_p=1/f_p$ ).

$$F_{nv}(t) = \sum_{k=0}^{\infty} F_n[\alpha(t - kT_p)] \quad (2)$$

$$F_{nl}(t) = \sum_{k=0}^{\infty} \{F_n[\alpha(t - 2kT_p)] - F_n[\alpha(t - (2k+1)T_p)]\} \quad (3)$$

$$\alpha = T_n / T_p \text{ or } \alpha = f_p / f_n \quad (1.8 \text{ Hz} \leq f_p < 2.2 \text{ Hz}) \quad (4)$$

Where  $\alpha$  is a time factor,  $f_n$  and  $T_n$  are the pacing rate and period ( $f_n=1/ T_n$ ) shown in Fig. 3 for normal walk.

In numerical analysis, the static load is modelled as ramp load in order to reduce the fluctuation of dynamic response at the beginning of time history analysis. It is assumed that the load density is 1.5 person per square meter and the average weight of a person is 700N, then the walking loads for normal walk ( $1.8 \text{ Hz} \leq f_p < 2.2 \text{ Hz}$ ) including vertical dynamic force (VDF)  $q_{nv}(t)$ , lateral dynamic force (LDF)  $q_{nl}(t)$  and vertical static (ramped) force (VSF)  $q_{sv}(t)$  can be modelled as:

$$q_{nv}(t) = 210F_{nv}(t) \quad (\text{N/m}^2) \quad (5a)$$

$$q_{nl}(t) = 8.4F_{nl}(t) \quad (\text{N/m}^2) \quad (5b)$$

$$q_{sv}(t) = \begin{cases} 840t/(10\alpha) & (\text{N/m}^2) & 0 < t < 10\alpha \\ 840 & (\text{N/m}^2) & t \geq 10\alpha \end{cases} \quad (5c)$$

Walking loads with other pacing rates can be similarly defined by following the same procedure.

## 4 Natural frequencies and vibration modes

Natural frequencies and corresponding vibration modes are important dynamic properties. When a bridge structure is under synchronous excitation, it vibrates on its own natural frequency and vibration mode and is subjected to resonant vibration.

In general, the structural stiffness of suspension bridges is mainly provided by the suspending cable system. The dynamic properties depend not only on the cable profile, but also on tension force in the cables, particularly for shallow suspension bridge structures, in which adjusting the cable tension and cable profiles can alter the vibration properties such as natural frequencies and mode shapes. In the proposed cable supported bridge structure with pre-tensioned bottom and/or side cables, if the pre-tension forces are introduced to the reverse profiled bottom cables, the tension forces in the top suspending cables will increase due to the extra internal vertical forces induced by the pre-tensioned bottom cables. If the side cables have been pre-tensioned, the horizontal structural stiffness will be improved greatly. Table 1 shows the maximum tension forces in the cable systems and frequencies as well as corresponding modes when different extra internal vertical forces are introduced into the pre-tensioned cables. In the analyses of these models the side cables were not considered.

Suspension bridges always have four main types of vibration modes<sup>22</sup>: lateral, vertical, torsional and longitudinal modes. A cable supported bridge structure (pre-tensioned or un-pre-tensioned) with shallow cable sag will also have these four types of vibration modes. However, numerical results show that the lateral modes and torsional modes do not always appear as pure lateral or torsional vibration modes. Often, they are combined together and form two types of coupled vibration modes: coupled lateral-torsional modes (LmTn) and coupled torsional-lateral modes (TmLn), where L and T represent lateral and torsional modes respectively and m and n are the

number of half waves. Results show that the coupled lateral-torsional vibration modes are dominated by the lateral vibration modes in conjunction with the torsional vibration, while coupled torsional-lateral modes are dominated by torsional vibration modes. Under some circumstance, the coupled mode will reduce to pure modes, particularly the coupled one half wave modes. Most vertical vibration modes appear as pure vertical modes, without corresponding lateral or torsional ones. The longitudinal modes are not listed in Table 1 as they are sensitive to the connection between the adjacent bridge frames and disappear from the first twenty frequencies when pre-tensions are introduced.

## **5 Resonant vibration under walking dynamic loads**

When a bridge structure is subjected synchronous excitation, the pacing rate of synchronized pedestrians is almost the same of one of the natural frequencies and the bridge vibrates in resonance. The vibrating mode depends on the distribution of dynamic loads and natural frequencies. In order to illustrate the dynamic characteristics of slender footbridges with coupled vibration modes under walking dynamic loads, the bridge model with the frequency of 0.75 Hz of first coupled lateral-torsional mode has been chosen for the dynamic analysis. In the numerical analysis, Hilber-Hughes-Taylor method<sup>20</sup> is used for the non-linear time history analysis under the walking dynamic loads, and it is assumed that the first and second modes (T1L1 and L2T2 or V1 and V2) have the same damping ratio. If it is not addressed in the following text, the damping ratio is always set to be 0.005. In the following text and discussion, the dynamic responses are picked up from two points to show the maximum dynamic responses. When the bridge resonates in the first modes (coupled and vertical), one of the cross member ends at the middle bridge fame is chosen as this point locates under the cable sag and the maximum deflection occurs at this location. If the bridge vibrates in the second modes, the one of the cross member ends of the bridge frame at the quarter span length is chosen for the maximum dynamic responses.

### **5.1 First coupled lateral-torsional mode (L1T1) and vertical mode (V1)**

The first coupled lateral-torsional mode (L1T1) and first vertical mode (V1) are easier to be excited by crowd loads than other vibration modes when the entire deck is full of pedestrians, as these two modes are one half wave symmetric vibration modes. While the first coupled torsional-lateral mode or torsional mode (T1) is not easy to be activated as the crowd loads are supposed to be distributed uniformly on the deck, although the first mode is also one half wave mode.

Fig. 4 shows the lateral and vertical dynamic deflections when the bridge resonates in the first coupled lateral-torsional mode (L1T1) under the walking dynamic loads (slow walk) at the frequency of 0.75 Hz. It can be seen that the amplitude of the lateral deflection increases to the maximum value, then decays and finally becomes constant, i.e., the vibration trends to be steady after several decays. While in the vertical direction, the vertical vibration amplitude is much smaller than the lateral one, though the vibration also trends to be steady after several decays. The vertical vibration is actually contributed by three parts: static load, vertical dynamic load and

the lateral sway of bridge frame under lateral dynamic load. It is evident that the bridge does not resonate in the vertical direction when subjected to the vertical dynamic load and the maximum vertical dynamic deflection is mainly produced by the resonant lateral sway. The details of dynamic deflections in steady vibration can be seen in the Fig. 5. Numerical results show that the curves of the lateral and vertical accelerations take the same dynamic features as their corresponding deflections. In practice, the steady vibration is more meaningful as the effect of initial conditions vanishes. The maximum steady deflections and accelerations are shown in Table 2. It can be seen that the maximum steady lateral dynamic deflection is about 0.0135m with acceleration of  $0.2942 \text{ m/s}^2$ , while maximum steady vertical deflection reaches 0.0169 m with acceleration of  $0.158 \text{ m/s}^2$ . The static lateral deflection under the static lateral force is about 0.0003m and then the dynamic amplification factor is almost 45 under resonant vibration.

When the first vertical mode (V1) is excited by the crowd loads at the frequency of 1.095 Hz, the bridge resonates mainly in the vertical direction and has small vibration in the lateral direction. Fig. 6 shows the lateral and vertical deflections. It can be seen that the lateral deflection is quite small and it is mainly induced by the lateral forces. In the vertical direction, the amplitude of vertical deflection increases gradually to steady value without decay and it is mainly contributed by the vertical dynamic forces. The maximum steady vertical deflection and acceleration reach about 0.1057 m and  $4.3706 \text{ m/s}^2$  (see Table 2) while the static vertical deflection is 0.0177m under the whole static vertical loads.

## 5.2 Other vibration modes

Other vibration modes can also be excited by crowds and these modes are mainly coupled lateral-torsional and coupled torsional-lateral modes. When the bridge deck is full of crowds, the vertical forces can remain the same, but the phase of lateral force at different location can be changed easily by the pedestrians when different mode is excited.

Table 2 shows the maximum steady deflections and accelerations of different vibration modes excited by crowds. Here, the dynamic responses of the second coupled modes (L2T2 and T2L2) are picked up from the one of the cross member ends of the frame at a quarter of span length from a bridge end, as the maximum lateral deflection happens at this location as mentioned before. It can be seen that when the first torsional-lateral mode (T1) is excited by crowds, the lateral deflection and acceleration are quite small, but the vertical deflection and acceleration are greater than those of other coupled modes as the mode is dominated by the torsion. Compared to the dynamic response of the second coupled modes L2T2 with T2L2, it can be seen that the lateral deflection and acceleration are greater in the L2T2 mode while the vertical deflection and acceleration are greater in the T2L2 mode. This is because L2T2 mode is dominated by lateral mode while T2L2 by torsional mode.

When pedestrians walk at the frequency (1.521 Hz) of second vertical mode (V2), the second vertical mode has not been excited but the first coupled lateral-torsional mode (L1T1). Since the vertical loads are distributed on the whole bridge deck, the load effect on the second vertical mode is not significant, but the frequency is close to that of the first coupled lateral-torsional mode (0.75 Hz and 1.50 Hz in the lateral and

vertical directions respectively). However, if the crowd loads are only distributed on a half span, both the L1T1 and V2 modes can be excited. Fig. 7 shows the dynamic lateral and vertical deflections at one of the ends of cross member at the quarter span length from a bridge end. From Table 2, it can also be seen that when the crowd loads are only distributed on half bridge span, the vertical deflection and acceleration is much greater than those when the loads are distributed on the whole bridge span.

### 5.3 Effect of damping

In general, damping has significant effect on dynamic responses and is the main control parameter in resonance. However, for the proposed shallow suspension footbridge model, the effect of damping on the dynamic responses is quite complex. Table 3 shows the peak values of deflections and accelerations in steady vibration under different damping ratio for the and first vertical mode (V1). It can be seen that the effect of damping on the first coupled lateral-torsional mode (L1T1) is different from that on the first vertical mode. It seems that the damping has only small effect on the first coupled lateral-torsional vibration mode. When the damping ratio increases from 0.002 to 0.02, the maximum lateral deflection only reduces from 0.0139 m to 0.01 m. However, the damping has significant effect on the vertical vibration. The maximum vertical deflection reduces from 0.1762 m to 0.0431 m and maximum vertical acceleration from  $7.7134 \text{ m/s}^2$  to  $1.396 \text{ m/s}^2$ .

### 5.4 Effect of static vertical loads

In the above numerical analysis, the crowd loads are modelled by equation 5, i.e. the loads are consisted of three parts as vertical dynamic force (VDF), lateral dynamic force (LDF) and vertical static force (VSF). In order to investigate the effects of different loads, particularly the vertical static load, the bridge model has been analysed under different load cases when it resonates in the first coupled lateral-torsional mode and first vertical mode. The load cases include pure lateral dynamic load LD (only LDF) or pure vertical dynamic load VD (only VDF), dynamic loads LVD (LDF and VDF), vertical loads VSD (VDF and VSF) and crowd loads LVS (LDF, VDF and VSF). Table 4 shows the maximum steady deflections and accelerations under different load cases. It can be seen that when the bridge mode vibrates in the L1T1 mode, the vertical dynamic load has only slight effect on the lateral deflection and acceleration, but when the vertical static force is taken into account, the lateral deflection and acceleration decrease significantly. While when the vertical mode V1 is excited, the effect of vertical static force is quite small. These effects can be shown more clearly in the view of dynamic amplitude and mean value. Table 5 shows the amplitudes and mean values under different load cases. For the mode of L1T1, the vertical static force has slight effect on the mean values of lateral deflection and acceleration, but significant effect on the amplitudes. For the mode of V1, the vertical static force has significant effect on the mean value of vertical deflection, but slight effect on the amplitudes of vertical deflection and acceleration. This phenomenon illustrates that for slender footbridge, the lateral vibration can be reduced by increasing the structural weight.

## 6 Conclusion

Due to the new technology and application of light and high strength materials, modern pedestrian bridges are designed and constructed slender and flexible. However, with low stiffness, structural mass and damping ratio, slender bridge structures are prone to vibration induced by pedestrians. If the natural frequencies of the bridge structures are within the frequency range of walking dynamic loads, they are easy to be subjected to synchronous excitations and serious vibration serviceability problems may arise.

In this paper, an innovative cable supported bridge model with pre-tensioned reverse profiled cables in vertical and horizontal planes is proposed to investigate the vibration characteristics of shallow suspension pedestrian bridge structures. The synchronous excitation is simulated by resonant vibration and the crowd walking dynamic loads have been modelled. Numerical results show that for shallow suspension bridge, the lateral and torsional vibration modes always combine together and form two types of coupled vibration modes: coupled lateral-torsional modes and coupled torsional-lateral modes. When the bridge resonates under walking dynamic loads, the dynamic behaviour in the lateral direction is quite different from that in the vertical direction. In the resonant vibration of coupled modes, the amplitude of lateral deflection and acceleration increase to the maximum values and decay, then the vibration tends to steady. However, in the resonant vibration of vertical modes, the amplitude of vertical deflection and acceleration increase gradually to constant value. It is found that for the proposed pre-tensioned cable supported bridge model, the damping has significant effect on the vertical vibration, but only small effect on the lateral vibration. Static vertical load has some function of suppressing lateral vibration.

## References

1. Bachmann H. "Lively" footbridges – a real challenge. *Proceedings of the International Conference on the Design and Dynamic Behaviour of Footbridges*, Paris, France, 2002, November 20-22.
2. Fujino Y., Pacheco B. M., Nakamura S. I. and Warnitchai P. Synchronization of human walking observed during lateral vibration of a congested pedestrian bridge", *Earthquake Engineering & Structural Dynamics*, 1993, **22**, No. 9, 741-758.
3. Fujino Y., Sun L., Pacheco B. M. and Chaiseri P. Suppression of horizontal motion by tuned liquid damper. *Journal of Engineering Mechanics*, 1992, **118**, 2017-2030.
4. Nakamura S. I. and Fujino Y. Lateral vibration on a pedestrian cable-stayed bridge. *Structural Engineering International: Journal of the International Association for Bridge and Structural Engineering (IABSE)*, 2002, **12**, No. 4, 295-300.
5. Nakamura S. I. Model for Lateral Excitation of Footbridges by Synchronous walking. *Journal of Structural Engineering*, 2004, **130**, No. 1, 32-37.
6. Dallard P., Fitzpatrick T., Flint A., Low A., Ridsdill Smith R. and Willford M. Pedestrian-induced vibration of footbridges. *The Structural Engineer*, 2000, **78**, No. 23/24, 13-17.

7. Dallard P., Fitzpatrick T., Flint A., Le Bourva S., Low A., Ridsdill Smith R. and Willford M. The Millennium Bridge, London: problems and solutions. *The Structural Engineer*, 2001, **79**, No. 8, 15-17.
8. Dallard P., Fitzpatrick A. J., Flint A., Le Bourva S., Low A., Ridsdill Smith R.M. and Willford M. The London Millennium footbridge. *The Structural Engineer*, 2001, **79**, No. 22, 17-32.
9. Dallard P., Fitzpatrick T., Flint A., Low A., Ridsdill Smith R., Willford M. and Roche M. London Millennium Bridge: pedestrian-induced lateral vibration. *Journal of Bridge Engineering*, 2001, **6**, No. 6, 412-416.
10. Pavic A., Willford M., Reynolds P. and Wright J. Key results of modal testing of the Millennium Bridge, London. *Proceedings of the International Conference on the Design and Dynamic Behaviour of Footbridges*, Paris, France, 2002, November 20-22.
11. Newland D. E. Vibration of London Millennium bridge: cause and cure. *International Journal of Acoustics and Vibration*, 2003, **8**, No. 1, 9-14.
12. Newland D. E. Pedestrian excitation of bridges – recent results. *Proceedings of Tenth International Congress on Sound and Vibration*, Stockholm, Sweden, 2003, July 7-10.
13. Blekherman A. N. Swaying of pedestrian bridges. *Journal of Bridge Engineering*, 2005, **10**, No. 2, 142-150.
14. Nakamura S. I. Field measurements of lateral vibration on a pedestrian suspension bridge. *The Structural Engineer*, 2003, **18**, November, 22-26.
15. Bachmann H. and Ammann W. *Vibrations in structures induced by man and machines*, IABSE-AIPC-IVBH, Switzerland, 1987.
16. Wheeler J. E. Prediction and control of pedestrian-induced vibration in footbridge. *Journal of Structural Division*, 1982, **108**, No. 9, 2045-2065.
17. Rainer J. H., Pernica G. and Allen D. E. Dynamic loading and response of footbridge. *Canadian Journal of Civil Engineering*, 1988, **15**, 66-71.
18. Kerr S. C. *Human induced loading on staircases*. PhD Thesis, Mechanical Engineering department, University College London, UK, 1998.
19. Andriacchi T. P., Ogle J. A. and Galante J.O. Walking speed as a basis for normal and abnormal gait measurements. *Journal of Biomechanics*, 1977, **10**, 261-268.
20. Computer and Structures, Inc. *CSI analysis reference manual*. Computer and Structures, inc., Berkeley, California, USA, September, 2004.
21. Willford M. Dynamic action and reaction of pedestrians. *Proceedings of the International Conference on the Design and Dynamic Behaviour of Footbridges*, Paris, France, 2002, November 20-22.
22. Xu Y. L., Ko J. M. and Zhang W. S. Vibration studies of Tsing Ma suspension bridge. *Journal of Bridge Engineering*, 1997, **2**, No. 4, 149-156.

## NOTATION

$A_l, A_v$	lateral and vertical accelerations
$A_{ul}, A_{uv}$	amplitude of lateral and vertical deflections
$A_{al}, A_{av}$	amplitude of lateral and vertical accelerations
$f_n$	pacing rate of normal walk
$F_n[t]$	force function of normal walk
$F_{nl}(t)$	continuous lateral force function
$F_{nv}(t)$	continuous vertical force function
$f_p$	pacing rate of walking load
$k$	integer number
L	lateral modes
LmTn	coupled lateral-torsional modes
LSWm	longitudinal swaying modes
m, n	number of half wave
$M_{ul}, M_{uv}$	mean value of lateral and vertical deflections
$M_{al}, M_{av}$	mean value of lateral and vertical accelerations
$q_{mv}(t)$	vertical dynamic force
$q_{nl}(t)$	lateral dynamic force
$q_{sv}(t)$	vertical ramped static force
$Q_{int}$	extra vertical force
$t$	time
T	torsional modes
$T_n$	period of normal walk
$T_{nc}$	contact time
$T_p$	period of walking load
TmLn	coupled torsional-lateral modes
$T_1, T_2, T_3$	tension force in top, bottom and side cables
$U_l, U_v$	lateral and vertical deflections
Vm	vertical modes
$W_{int}$	extra vertical force
$\alpha$	time factor

## ABBREVIATION

LD	pure lateral dynamic load
LDF	lateral dynamic force
LVD	dynamic loads consisting of lateral and vertical dynamic forces
LVS	crowd loads consisting of lateral, vertical dynamic force and vertical static force
VD	pure vertical dynamic load
VDF	vertical dynamic force
VSF	vertical (ramped) static force

## **LIST OF FIGURES**

- Fig. 1. Pre-tensioned cable supported bridge model: (a) – elevation; (b) – top view; (c) – middle transverse bridge frame
- Fig. 2. Typical vertical force patterns of walk activities
- Fig. 3. Force function of normal walk
- Fig. 4. Lateral and vertical deflections of the first coupled lateral-torsional mode: (a) – lateral; (b) – vertical
- Fig. 5. Dynamic deflections in detail of the first coupled lateral-torsional mode
- Fig. 6. Resonant lateral and vertical dynamic deflections of mode V1 (1.095 Hz): (a) – lateral deflection; (b) – vertical deflection
- Fig. 7. Deflections under walking loads (1.521 Hz) distributed on half bridge span (a) – lateral deflection; (b) – vertical deflection

## **LIST OF TABLES**

- Table 1. Internal force via natural frequencies and corresponding modes
- Table 2. Maximum deflections and accelerations at different vibration modes
- Table 3. Effect of damping on the dynamic responses
- Table 4. Maximum deflections and accelerations under different load cases
- Table 5. Amplitudes and mean values of deflections and accelerations under different load cases

## Figures

Fig. 1(a)

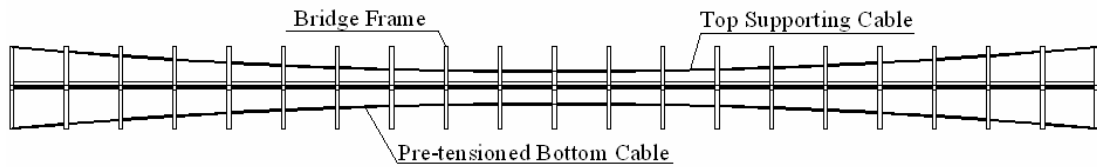


Fig. 1(b)

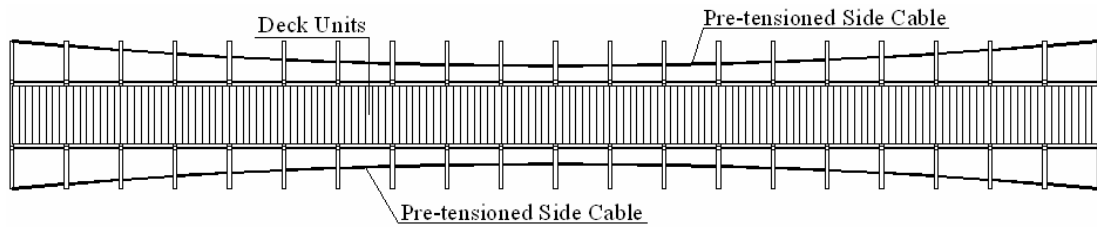


Fig. 1(c)

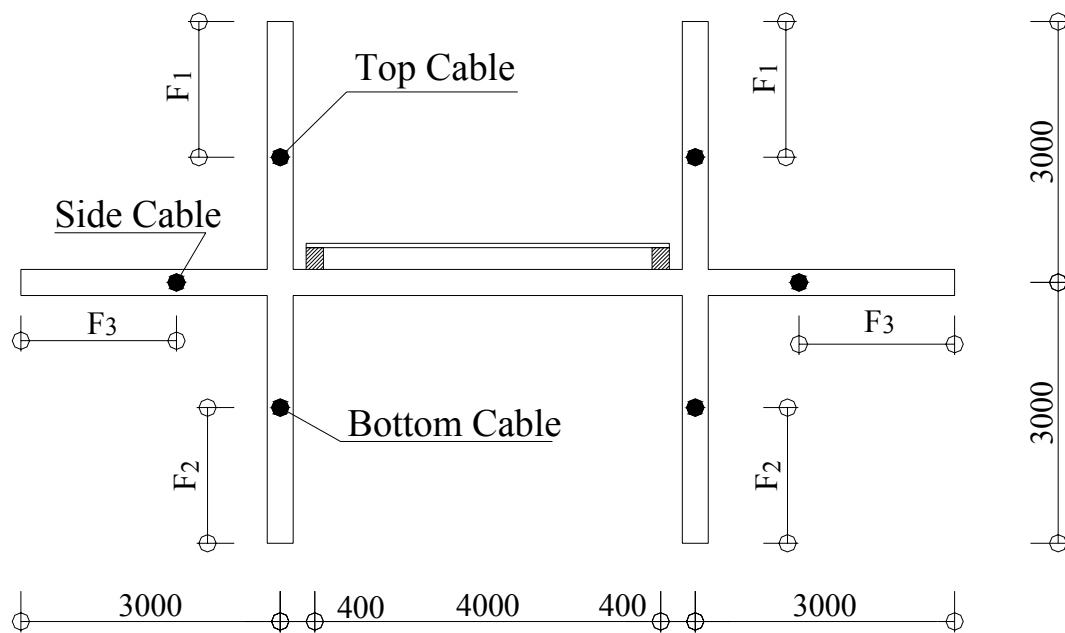


Fig. 2

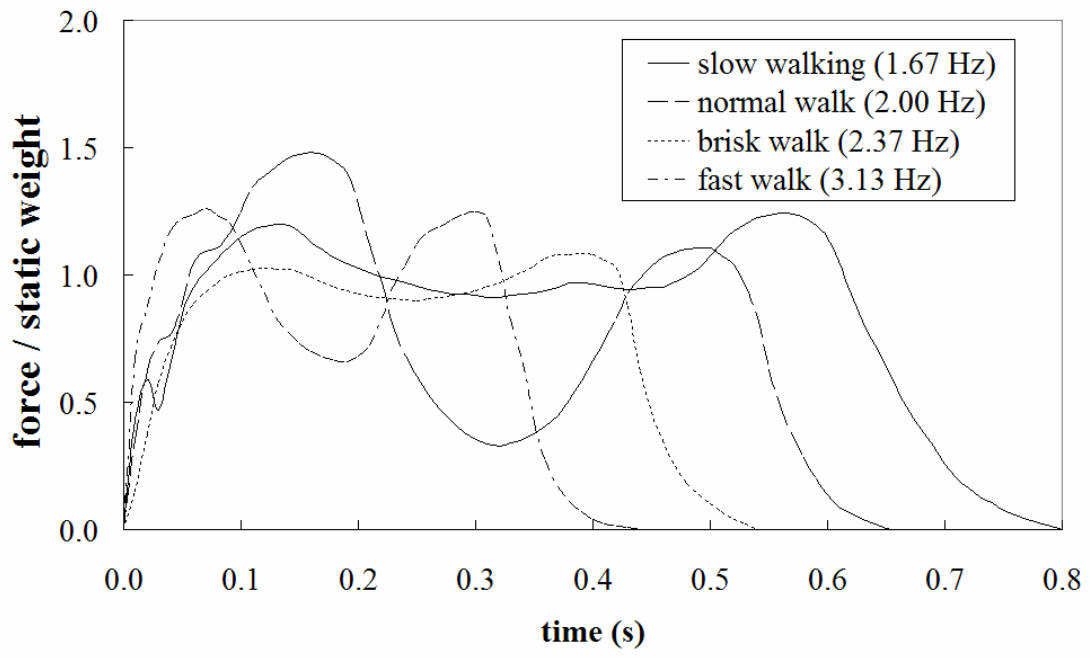


Fig. 3

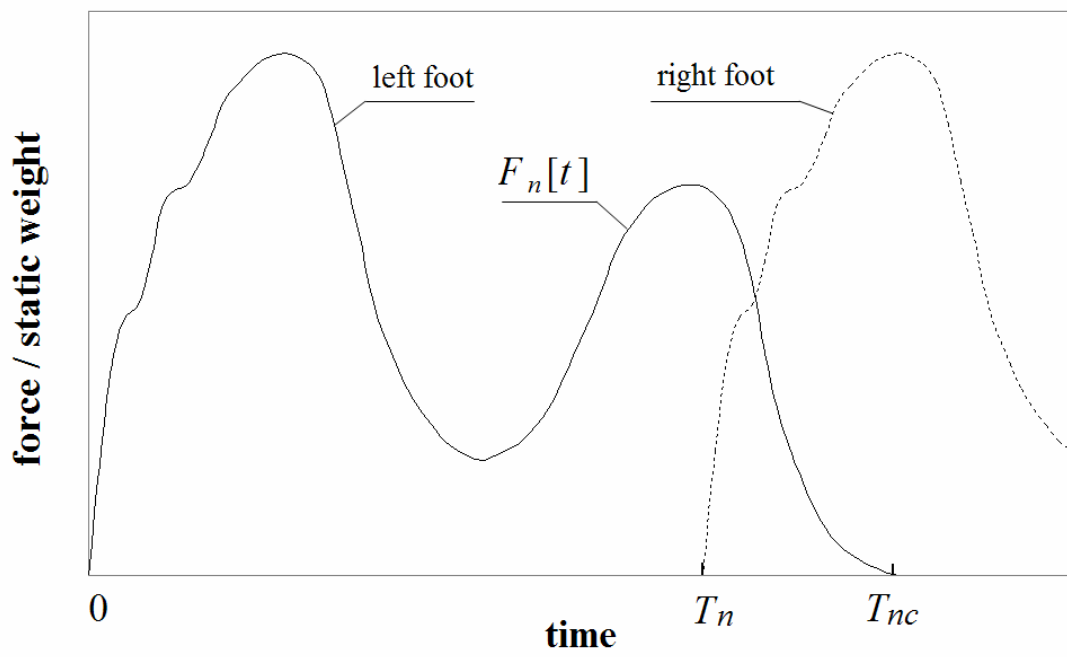


Fig. 4(a)

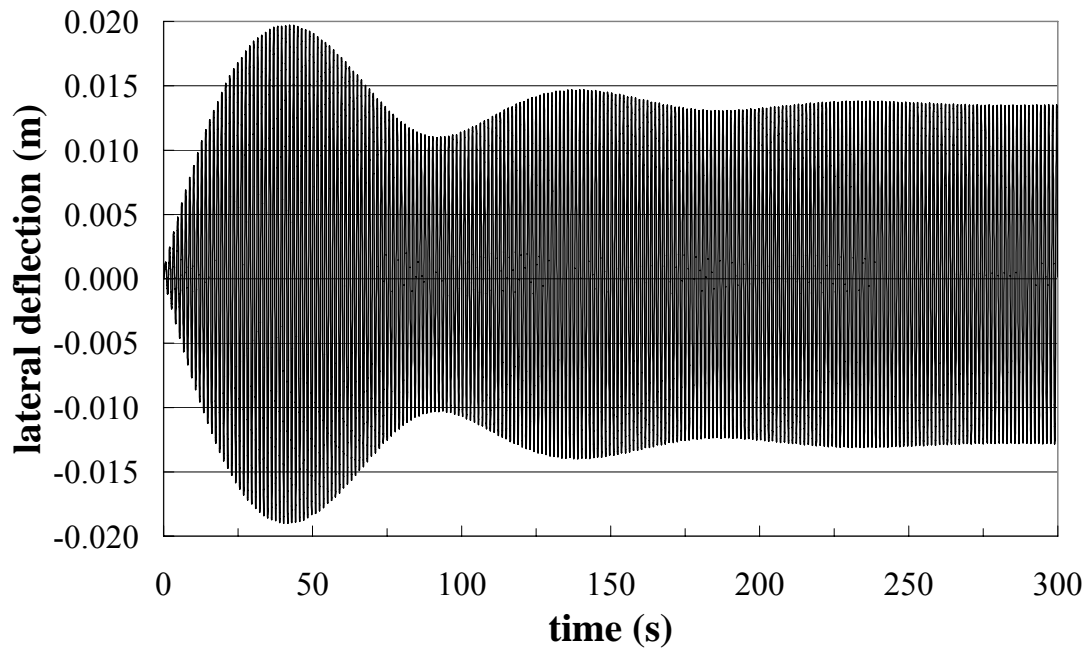


Fig. 4(b)

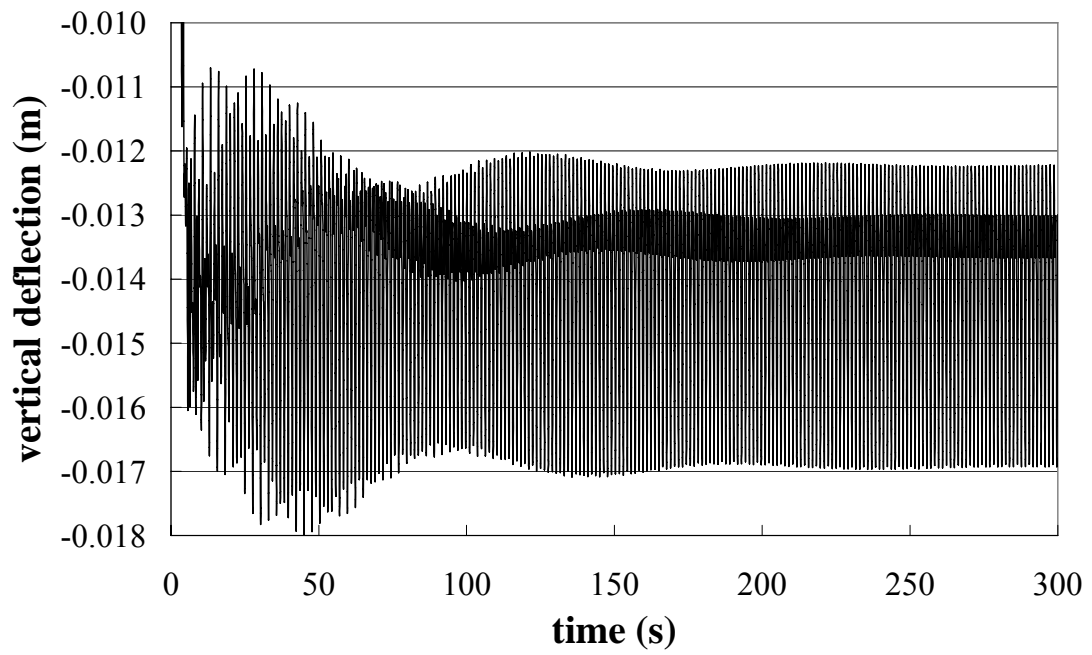


Fig. 5

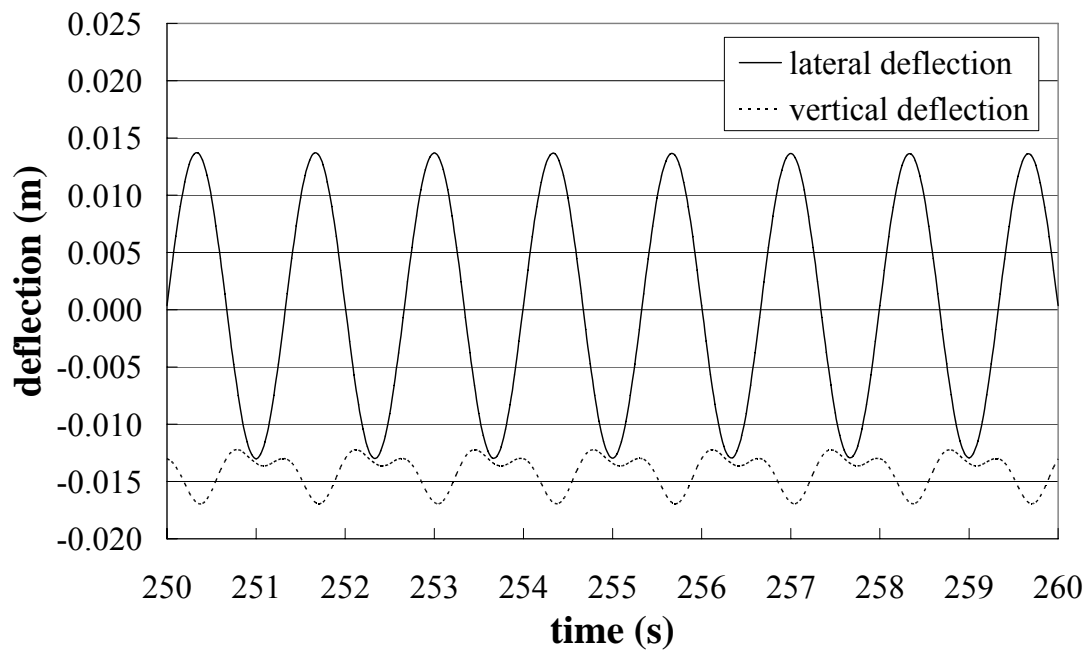


Fig. 6(a)

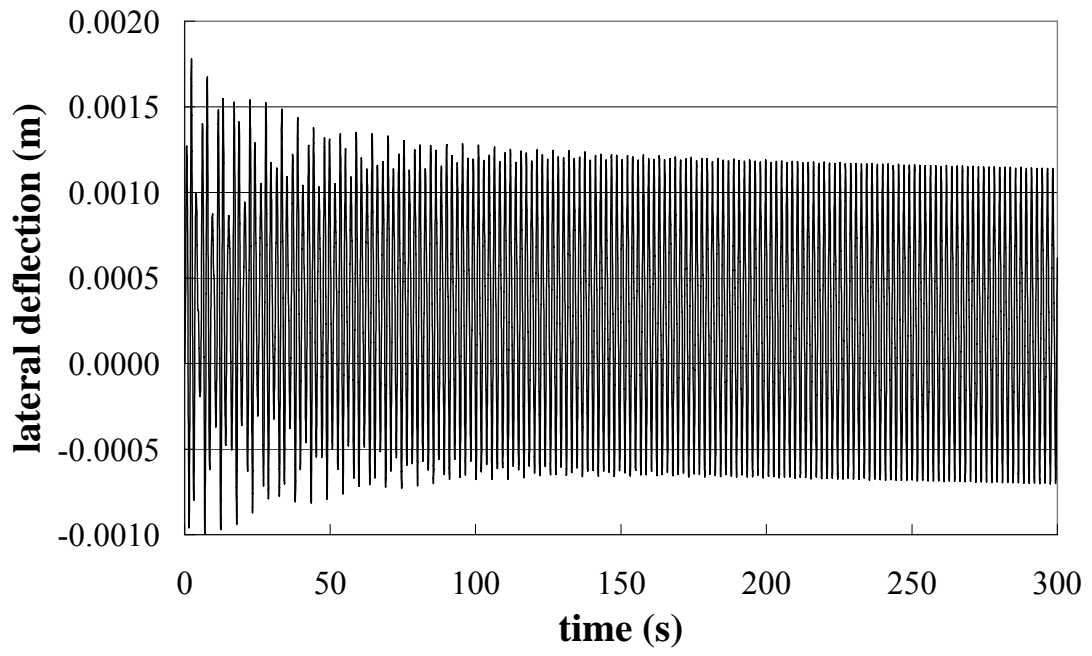


Fig. 6(b)

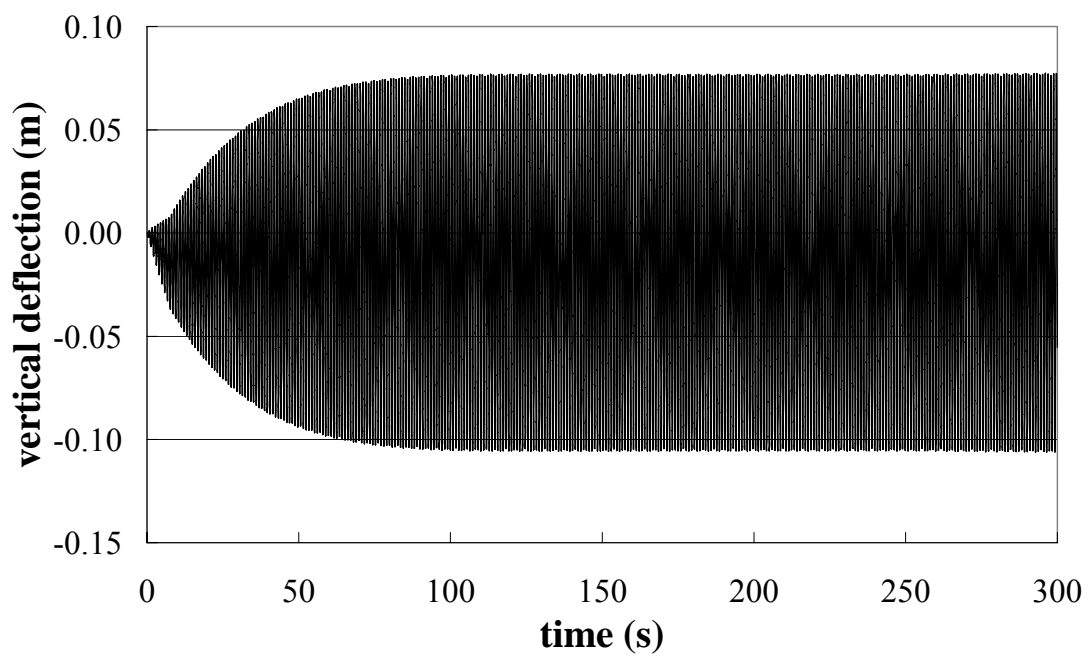


Fig. 7(a)

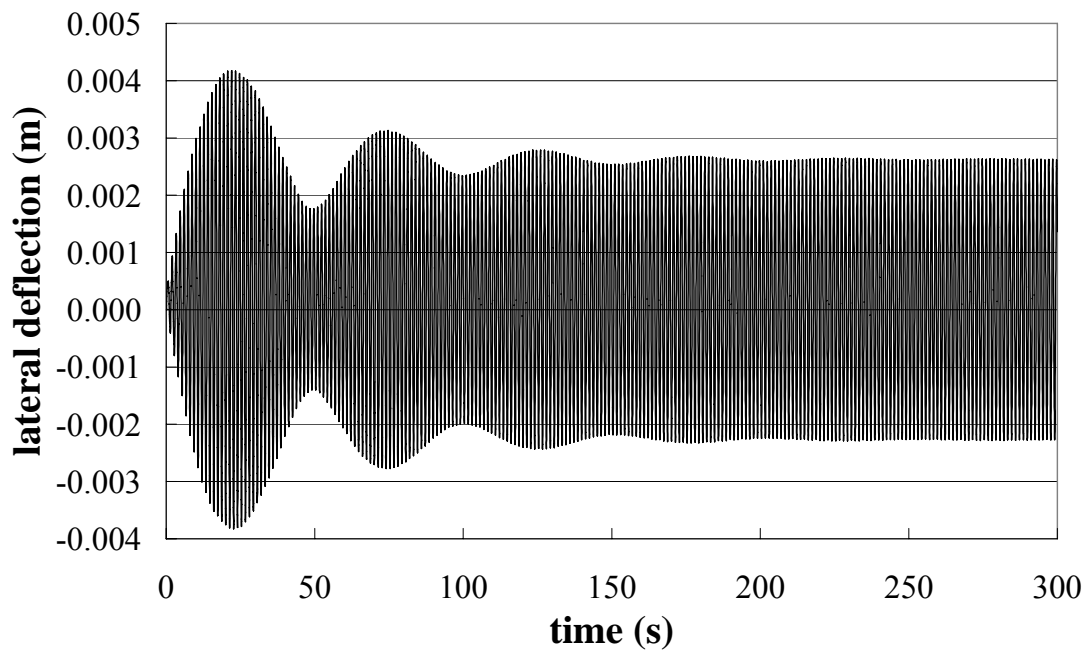
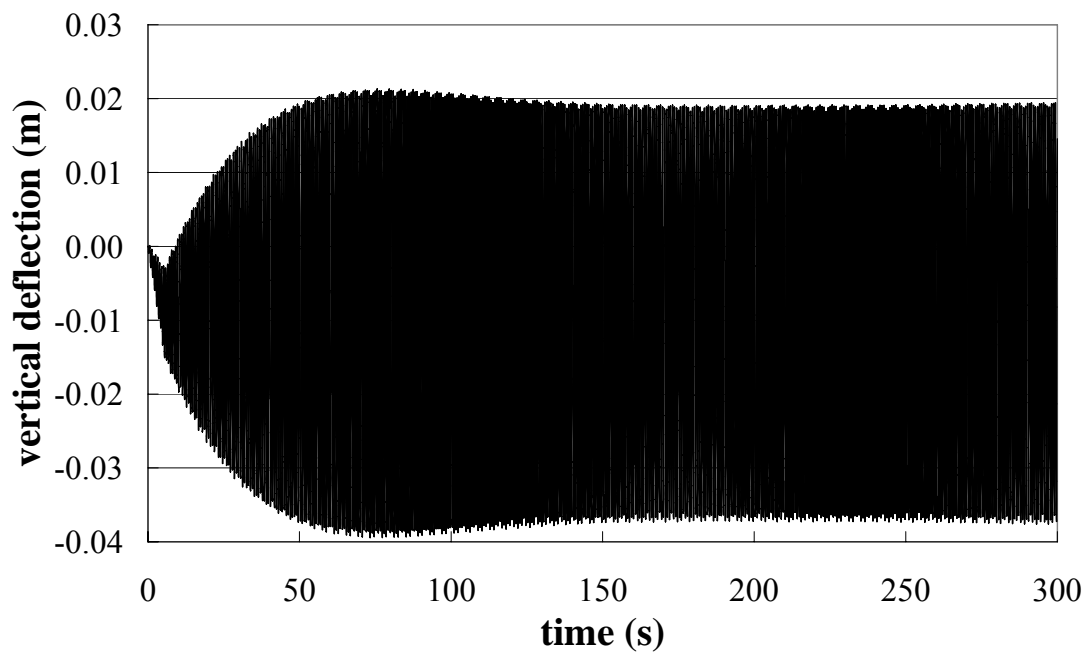


Fig. 7(b)



## Tables

Table 1. Internal force via natural frequencies and corresponding modes

Maximum Tension forces	T <sub>1</sub> (N)	1.64E+07	2.05E+07	2.82E+07
	T <sub>2</sub> (N)	3.01E+06	7.15E+06	1.49E+07
	T <sub>3</sub> (N)	0	0	0
Coupled Lateral-Torsional	L1T1	0.500	0.600	0.750
	L2T2	0.862	1.096	1.426
	L3T3	1.248	1.604	2.102
	L4T4	1.631	2.108	2.771
	L5T5	2.024	2.617	3.437
	L6T6	2.374	3.119	4.089
Coupled Torsional-Lateral	T1	0.860	0.938	1.064
	T2L2	1.253	1.424	1.697
	T3L3	1.845	2.098	2.497
	T4L4	2.458	2.756	3.283
Vertical	V1	0.927	0.992	1.095
	V2	1.033	1.227	1.521
	V3	1.572	1.856	2.290
	V4	2.055	2.442	3.026
	V5	2.568	3.049	3.775

Table 2. Maximum deflections and accelerations at deferent vibration modes

Mode	L1T1	T1	V1	L2T2	T2L2	V2 <sup>*</sup>	V2 <sup>+</sup>
Frequency (Hz)	0.750	1.064	1.095	1.426	1.697	1.521	1.521
Activity	slow walk	normal walk	slow walk	fast walk	fast walk	slow walk	slow walk
U <sub>ld</sub> (m)	0.0135	0.0008	0.0011	0.0027	0.0016	0.0052	0.0026
U <sub>vd</sub> (m)	-0.0169	-0.0183	-0.1057	-0.0122	-0.0130	-0.0116	-0.0373
A <sub>ld</sub> (m/s <sup>2</sup> )	0.2942	0.0247	-0.0172	0.2220	-0.1817	0.1088	0.0532
A <sub>vd</sub> (m/s <sup>2</sup> )	0.1580	0.6261	4.3706	0.2290	0.3791	-0.1075	-2.5549

Note: <sup>\*</sup> - crowd loads distributed on full span; <sup>+</sup> - crowd loads distributed on half span

Table 3. Effect of damping on the dynamic responses

Mode	L1T1 (0.750 Hz)				V1 (1.095 Hz)			
	0.002	0.005	0.010	0.020	0.002	0.005	0.010	0.020
U <sub>l</sub> (m)	0.0139	0.0135	0.0125	0.0100	0.0010	0.0011	0.0012	0.0012
U <sub>v</sub> (m)	-0.0170	-0.0169	-0.0166	-0.0163	-0.1762	-0.1057	-0.0675	-0.0431
A <sub>l</sub> (m/s <sup>2</sup> )	0.3145	0.2942	0.2712	0.2124	0.0154	0.0172	0.0172	0.0173
A <sub>v</sub> (m/s <sup>2</sup> )	0.1694	0.1580	0.1517	0.1475	7.7134	4.3706	2.5587	1.3960

Table 4. Maximum deflections and accelerations in steady vibration

mode	LIT1			V1			
load case	LD	LVD	LVS	VD	LVD	VSD	LVS
$U_l$ (m)	0.01481	0.014768	0.013501	8.86E-09	0.001189	6.42E-09	0.001141
$U_v$ (m)	-0.00178	-0.00285	-0.01694	-0.09182	-0.09171	-0.10573	-0.1069
$A_l$ (m/s <sup>2</sup> )	0.32345	0.32262	0.29420	5.09E-05	0.01667	5.28E-05	0.0115
$A_v$ (m/s <sup>2</sup> )	0.04637	0.16262	0.15798	4.39184	4.38365	4.37933	4.37058

Table 5. Amplitudes and mean values of deflections and accelerations in steady vibration

mode	LIT1			V1			
load case	LD	LVD	LVS	VD	LVD	VSD	LVS
$A_{ul}$ (m)	0.0145	0.0144	0.0131	0.0000	0.0009	0.0000	0.0009
$M_{ul}$ (m)	0.0004	0.0004	0.0004	0.0000	0.0003	0.0000	0.0003
$A_{uv}$ (m)	0.0018	0.0025	0.0023	0.0916	0.0915	0.0914	0.0913
$M_{uv}$ (m)	0.0000	-0.0004	-0.0146	-0.0002	-0.0002	-0.0144	-0.0144
$A_{al}$ (m/s <sup>2</sup> )	0.3232	0.3224	0.2938	0.0001	0.0172	0.0001	0.0174
$M_{al}$ (m/s <sup>2</sup> )	0.0002	0.0002	0.0004	0.0000	-0.0005	0.0000	-0.0002
$A_{av}$ (m/s <sup>2</sup> )	0.0466	0.1532	0.1511	4.3423	4.3346	4.3299	4.3217
$M_{av}$ (m/s <sup>2</sup> )	-0.0002	0.0094	0.0069	0.0496	0.0491	0.0494	0.0489